Biological Journal of the Linnean Society, 2018, **XX**, 1–9. With 6 figures.

Use of three-dimensional geometric morphometrics for the identification of closely related species of Caucasian rock lizards (Lacertidae: *Darevskia*)

MARIAM GABELAIA[1], DAVID TARKHNISHVILI[1] and DOMINIQUE ADRIAENS[2]

[1]*Ilia State University, School of Natural Sciences and Engineering, Kakutsa Cholokashvili Ave 3/5, Tbilisi, 0162, Georgia*
[2]*Ghent University, Evolutionary Morphology of Vertebrates, K. L. Ledeganckstraat 35, Gent 9000, Belgium*

Received 11 June 2018; revised 28 August 2018; accepted for publication 28 August 2018

Geometric morphometrics is a better tool to evaluate the variation of shape than 'traditional' morphometrics. In reptiles, it outperforms morphometrics based on linear measurements and scalation. In an earlier study, two-dimensional outline-based geometric morphometrics in six species of rock lizards (*Darevskia*) showed that their shapes reflected the species divergence pattern. This allowed us to separate species from different clades, but we could not distinguish closely related species within a clade. We hypothesized that three-dimensional (3D) head shape data would be sufficiently discriminative to identify closely related species. To test this hypothesis, we compared head shapes of three closely related species of the '*rudis*' clade, *Darevskia portschinskii*, *Darevskia valentini* and *Darevskia rudis*, with the last species treated as two distinct groups (*D. r. obscura* vs. *D. r. rudis*), using 3D landmark data. The 3D analysis isolated the species of the '*rudis*' clade from each other and even separated individuals from populations that showed a genetic introgression pattern. The analysis showed that *D. r. obscura* is morphologically as distinct from *D. r. rudis* as from the other nominal species. For this reason, we suggest elevating the status of *D. r. obscura* to species level, i.e. *Darevskia obscura* Lantz & Cyrén, 1936.

ADDITIONAL KEYWORDS: head shape – species boundaries – three-dimensional photogrammetry.

INTRODUCTION

Caucasian rock lizards (genus *Darevskia* Arribas, 1999) are a small-bodied, speciose group of rock lizards mostly found in the Caucasus (Darevsky, 1967; Tarkhnishvili, 2012). This group is composed of three ('*rudis*', '*caucasica*' and '*saxicola*') matrilineal clades, each consisting of several species, according to Murphy *et al.* (2000). The scalation pattern in *Darevskia* is highly variable at the individual level, with individual scalation traits strongly overlapping among the species. As such, there are no fully diagnostic scalation differences for most of the *Darevskia* species (Darevsky, 1967; Tarkhnishvili, 2012).

Geometric morphometrics (GM) has been proved to assess shape variation better than 'traditional' (linear measure based) morphometrics (Rohlf & Marcus, 1993; Zelditch *et al.*, 2004; Blanco & Godfrey, 2006; Bernal, 2007; Maderbacher *et al.*, 2008; Abdel-Rahman *et al.*, 2009; Breno *et al.*, 2011; Schwarzfeld & Sperling, 2014). In a previous study, Gabelaia *et al.* (2017) used GM techniques, more specifically outline-based elliptic Fourier analysis, for comparing and identifying rock lizards from different clades based on the anal and pileus scales. Gabelaia *et al.* (2017) focused on six species from the '*rudis*' and '*caucasica*' clades. The analysis separated individuals from different clades and produced a dendrogram congruent with a species-level molecular phylogeny (Murphy *et al.*, 2000; Tarkhnishvili, 2012) but was unable to distinguish between closely related species within the same clade.

In the present work, we hypothesized that the application of GM on lizard head shape, which contributes to more evolutionarily informative data (Kaliontzopoulou *et al.*, 2007), would provide a more powerful dataset on species-specific variation, especially when quantified in three dimensions (3D), and this would allow discrimination between closely related species. Starting from the 2000s, the use of 3D GM has increased in studies that examine patterns of organismal morphological variation (Goricki & Trontelj, 2006; Sztencel-Jabłonka *et al.*, 2009;

---

*Corresponding author. E-mail: mariam.gabelaia.1@iliauni.edu.ge

Adams *et al.*, 2013; Ivanovic *et al.*, 2013; Mangiacotti *et al.*, 2014; Gray *et al.*, 2017). The advantage of 3D GM compared with 'traditional' morphometrics and/or two-dimensional (2D) GM is that not only does it capture subtle shape variation in more detail, but also it allows a better visualization of that variation (Zelditch *et al.*, 2004; Klingenberg, 2013). For this study, we analysed head shape variation in three closely related species of the '*rudis*' clade: *Darevskia rudis* Bedriaga, 1886 (including the subspecies *Darevskia rudis obscura* and *Darevskia rudis rudis*); *Darevskia portschinskii* Kessler, 1878 and *Darevskia valentini* Boettger, 1892 (Murphy *et al.*, 2000; Tarkhnishvili, 2012). The respective evolutionary lineages of the '*rudis*' clade species separated from a common ancestor supposedly during the late Pleistocene and are still in a stage of incomplete lineage sorting (Tarkhnishvili *et al.*, 2013). *Darevskia rudis* is found in most of the Caucasus and Asia Minor, whereas *D. valentini* replaces *D. rudis* in the south of the Lesser Caucasus (Fig. 1). In the central part of the Lesser Caucasus, only *D. portschinskii* is found. Hence, the species are parapatrically distributed and form contact zones (Tarkhnishvili, 2012; Tarkhnishvili *et al.*, 2013). This parapatrical distribution explains the broad gene introgression zone between *D. portschinskii* and *D. r. obscura*. Another form, *Darevskia rudis macromaculata*, is found in some locations geographically close to the range of *D. r. obscura* (Darevsky, 1967) and belongs to the same monophyletic mitochondrial clade as *D. r. obscura* (Tarkhnishvili *et al.*, 2013). This clade is equidistant from *D. portschinskii*, *D. valentini* and *D. r. rudis* (Tarkhnishvili *et al.*, 2013). Arribas *et al.* (2013) suggested a conspecific status for all forms within *D. rudis* and synonymized *D. r. macromaculata* with *D. r. obscura*.

The three species investigated in this study (*D. rudis*, *D. valentini* and *D. portschinskii*) differ in body size, colour pattern and some scalation traits. Adult *D. r. rudis* have a larger body than adult *D. portschinskii*, with *D. valentini* (together with the subspecies *D. r. obscura*) being larger than *D. portschinskii* but smaller than most of the *D. r. rudis* populations (Darevsky, 1967). *Darevskia valentini* has a brighter coloration compared with the other species, with large contrasting dark spots on the back. All subspecies of *D. rudis* have shin scales markedly larger than the dorsal scales, different from the other species of the clade, whose shin scales are not larger than the dorsal scales (Darevsky, 1967; Tarkhnishvili, 2012).

In this work, we aimed to compare 3D head shape variation between *D. portschinskii*, *D. valentini* and *D. rudis* by collecting 2D images from lizards that were then used to generate 3D meshes through photogrammetry. The last of these species was treated as two groups: *D. r. obscura* and *D. r. rudis*. Using 3D landmark data, we aimed to determine whether 3D morphometrics provides more reliable diagnostic information that could separate the studied taxa than the 2D outline data on scalation patterns used before (Gabelaia *et al.*, 2017) or 'traditional' analysis of scalation applied to the same taxonomic groups (Darevsky, 1967; Tarkhnishvili *et al.*, 2013).

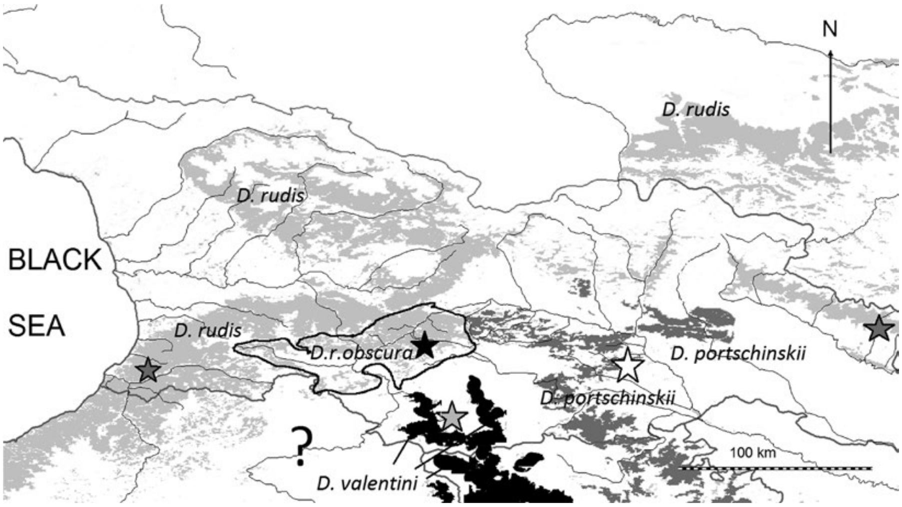

Figure 1. The distribution (according to Darevsky, 1967; Tarkhnishvili *et al.*, 2013) of the studied taxa in the Central and Western Caucasus. The ranges of *Darevskia rudis* (light grey areas) and *Darevskia portschinskii* (dark grey areas) coincide with the distribution of mountain forests. The distribution of *Darevskia valentini* (black area) is along the valleys of the major rivers and in the Abul-Samsari mountain range in southern Georgia. The range of *D. r. obscura* is delimited with a thick line. The question mark shows the area in NE Turkey where we refrain from naming the exact taxon of the *D.* '*rudis*' clade (most probably *D. r. obscura* or *D. valentini*). The stars indicate sampling locations (Table 1).

Table 1. Sample size and sampling locations of the *Darevskia* specimens studied

Taxon	Samples	Location	Geographical coordinates
D. portschinskii	3♂ 8♀	Kojori	41.649N 44.683E
D. rudis obscura	8♂ 3♀	Borjomi	41.873N 43.411E
D. rudis rudis	6♂ 10♀	Charnali 2♂ 5♀ Lagodekhi 4♂ 5♀	41.554N 41.607E 41.855N 46.300E
D. valentini	7♂ 4♀	Akhalkalaki	41.301N 43.389E

MATERIAL AND METHODS

We collected 49 adult (male and female) individuals from five locations in Georgia. Single sites were sampled for *D. portschinskii*, *D. valentini* and *D. r. obscura*; and two sites were sampled for *D. r. rudis*, including the south-west and the north-east of Georgia (Fig. 1; Table 1). All five locations/populations were studied earlier using mitochondrial DNA sequencing and microsatellite genotyping (Tarkhnishvili *et al.*, 2013); hence, their attribution to one of the four studied taxa had been genetically validated. Each individual was anaesthetized using chloroform. The individual was positioned in the centre of a cardboard circle in a tube with its head pointed upwards; the head was then photographed 36 times from a perspective of 90° to the midline and 36 times from a perspective of 45° to the midline, by moving the camera around the lizard (Fig. 2). Images were uploaded in AgiSoft PhotoScan Pro v.1.2.6 (Agisoft, 2016), which first aligned the images in 3D spaces and then generated 3D models of the head surface, onto which 66 homological landmarks were subsequently digitized (Fig. 3; Supporting Information, Appendix S1).

After digitizing the landmarks in AgiSoft PhotoScan Pro v.1.2.6, we exported the 3D coordinates in a DXF (drawing exchange format) and arranged them in Microsoft Excel (Microsoft Corporation, 2007) to retain landmark names and coordinates. We aligned and scaled 3D coordinates by performing a Procrustes superimposition using the software PAST (Hammer *et al.*, 2001). Aligned and scaled coordinates were then used for principal components analysis (PCA) in PAST (Hammer *et al.*, 2001). The individual scores along the meaningful principal component (PC) axes (obtained through a broken-stick analysis; Jackson, 1993) were used for the ordination of the individuals, in order to explore overall shape variation and to infer whether the axes already differentiated between the studied taxa.

To test for group differences in head shape, given that parametric test assumptions were not met, we applied a nonparametric (NP) MANOVA (Cooley & Lohnes, 1971) to seven meaningful PC scores. This method did not reveal significant differences in the head shape 3D data between the males and the females ($P > 0.05$); therefore, the sexes were pooled for the further analyses. We then applied the NP-MANOVA on two levels of grouping: the three nominal species (*D. portschinskii*, *D. valentini* and *D. rudis*), and these nominal species with *D. r. obscura* treated as a separate taxon (*D. portschinskii*, *D. valentini*, *D. r. rudis* and *D. r. obscura*). We included *D. r. obscura* as a separate taxon for two reasons: its monophyletic matrilineal origin, and the preliminary general PCA results showing that individuals of *D. r. obscura* grouped separately from those of *D. r. rudis* (see the Results section). Post-hoc tests (Hotelling's *P*-values and Bonferonni-corrected *P*-values) were performed to determine whether the differences were significant for each level of grouping.

As an ordination to visualize the levels of between-group differences in head shape between the four taxa, both a canonical variate analysis (CVA) and a between-group PCA (BG-PCA) were performed. To avoid ordination bias in the CVA owing to the low sample size per group (compared with the high number of variables), the CVA was done on the scores of the seven meaningful PCs (the robustness of the CVA was verified through a classifier analysis, combined with confusion matrix analysis, showing that the a priori grouping was well supported by the shape data). The BG-PCA was performed on the total landmark coordinates dataset. All these analyses were done in PAST (Hammer *et al.*, 2001).

To visualize which shape patterns were reflected in these ordinations, and thus which were the most discriminating shape differences between groups, we generated landmark wireframes that reflect canonical variate (CV) axis variation from a CVA on the total dataset of the 66 original landmarks in MorphoJ

(Klingenberg, 2011). Given that the orientations of the CV axes (with respect to the taxa group means) in this CVA were similar to those of the CVA on the meaningful PCs, the wireframes could be used to represent group differences as obtained through the latter CVA.

To check whether 3D GM analysis is more powerful in differentiating closely related lizard species than 2D GM study using outlines, we repeated the analysis described by Gabelaia *et al.* (2017) for all specimens described in the present paper. We conducted a Fourier outline shape analysis on the anal scale, which was shown to be the most effective approach for distinguishing evolutionary lineages of rock lizards, compared with other methods, including the analysis of the dorsal view of the head (Gabelaia *et al.*, 2017). We applied a NP-MANOVA and CVA on the 'meaningful' PCs to compare the results with 3D GM results.

All procedures with live animals were ethically approved by the Ilia State University Commission for Ethical Issues and were in accordance with Article 259 of Georgian Criminal Law. General anaesthesia of the lizards was used to avoid killing the animals collected in the wild. After photographing, the lizards were released to their natural habitats.

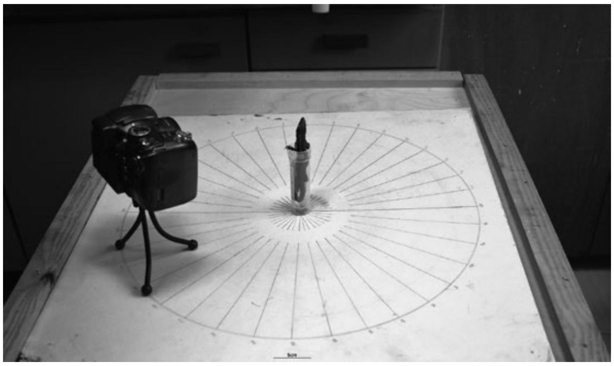

Figure 2. Set-up used for photographing the head of an immobilized lizard. The circle indicates the different positions at which a picture was taken.

RESULTS

The first seven PCs explained 62% of the overall shape variation (for eigenvalues and character loadings, see Supporting Information, Appendix S2). The first PC axis clearly discriminated between *D. r. obscura* and *D. r. rudis*. This axis also separated *D. portschinskii* and *D. r. rudis*. The first and the second axes showed different average scores between the studied taxa (Fig. 4). The NP-MANOVA confirmed significant differences between the taxa for both levels of groupings. Higher *F*-values were obtained for the analysis where *D. r. obscura* was included as a separate taxon ($F_{3,48} = 12$ vs. $F_{2,48} = 8.8$; $P < 0.05$ in both cases), which means higher overall differentiation among the taxa. The post-hoc tests, both uncorrected and Bonferonni-corrected Hotelling's *P*-values, confirmed significant

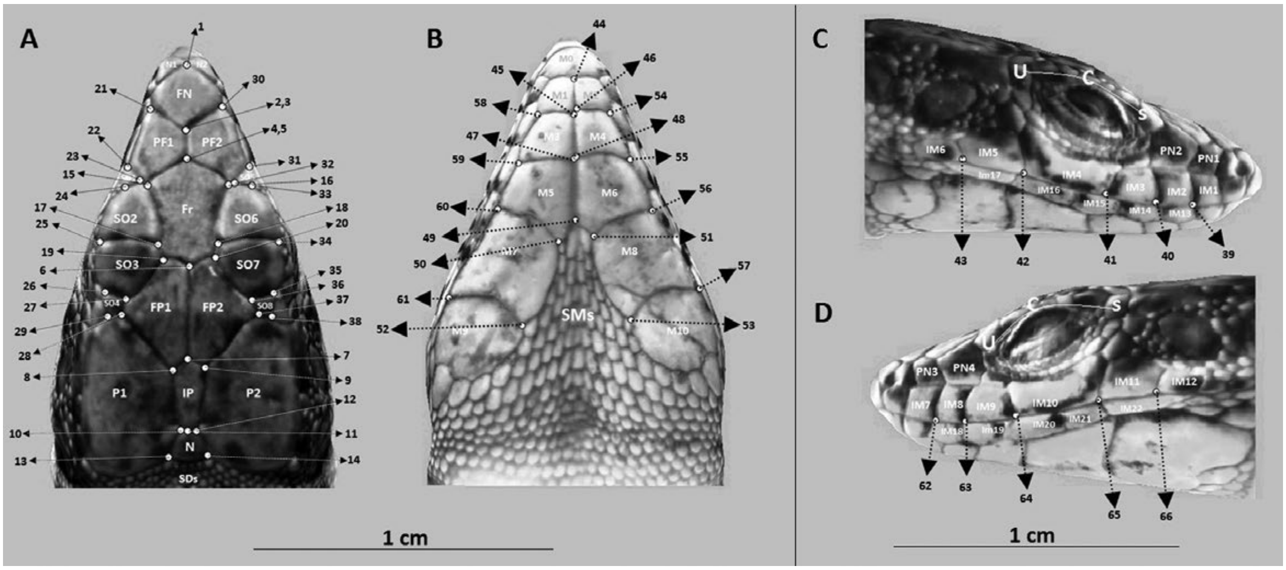

Figure 3. Digitized three-dimensional landmarks. Names of the scales are indicated with white text, and landmarks are identified with black numbers (see description of the scales and landmarks in Supporting Information, Appendix S1). A, dorsal view of the head. B, ventral view of the head. C, view of the right profile of the head. D, view of the left profile of the head. The specimen in the photograph is *Darevskia rudis rudis*.

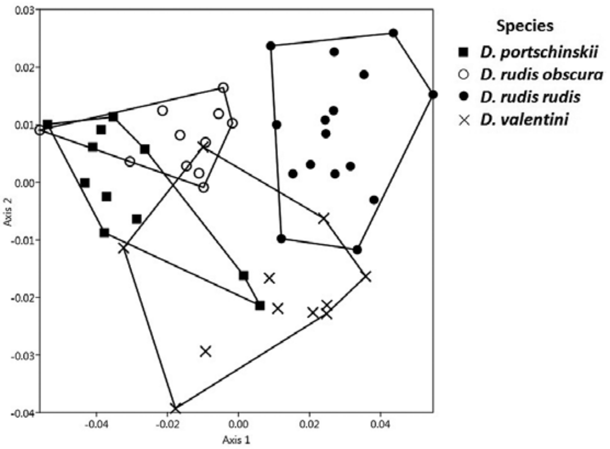

Figure 4. Plot of the first axis vs. the second axis from the principal components analysis on the three-dimensional head shape of the *Darevskia* lizards, analysing all 66 landmarks.

differences ($P < 0.05$) for each pairwise comparison across the four included taxa.

The BG-PCA axes completely separated all four studied taxa (Fig. 5A, B). The first axis (explaining 67% of the variation) fully separated *D. r. rudis* from *D. r. obscura* and from *D. portschinskii*. The second axis (19% of the variation) fully separated *D. valentini* from *D. r. rudis* and from *D. r. obscura*. The third axis (14% of the variation) fully separated *D. r. obscura* from *D. portschinskii*. Plotting the first axis vs. the third axis fully separated *D. portschinskii* from *D. valentini*.

The CVA based on seven meaningful PCs (PC_CVA) and CVA based on the Procrustes coordinates of all 66 landmarks (LM_CVA) discriminated the four taxa. The orientations of the first axis (CV1) and the third axis (CV3) from both the PC_CVA and LM_CVA coincided, whereas that of the second axis (CV2) showed opposite directions (see plots in Supporting Information, Appendix S3). For the PC_CVA, CV1 fully separated *D. r. rudis* from *D. portschinskii* and *D. valentini* (explaining 58.5% of the variation), CV2 (28.5% of the variation) separated *D. valentini* from *D. portschinskii*, and CV3 (13% of the variation) partly separated *D. valentini* from *D. r. obscura*. Combining CV1 with CV2 showed a complete separation of *D. r. obscura* and *D. portschinskii*, whereas *D. r. obscura* was separated from *D. r. rudis* when plotting CV1 vs. CV3. The confusion matrix classified 96% of the individuals correctly; after jackknifing, the preciseness of classification went down to 86% of the individuals (see Supporting Information, Appendix S4). In summary, discrimination in the PC_CVA was incomplete only for *D. r. obscura* and *D. valentini*, but completely separated all other taxa (Supporting Information, Appendix S3).

Group differences explained by CV1 included differences in snout length, head height, width at the level of the jaw joint and the size of interparietal (IP) scale (Fig. 6A). Individuals with lower CV1 scores have a taller and narrower head in the jaw joint area and a smaller IP scale (especially *D. r. rudis*), whereas individuals with high CV1 scores have a flatter and wider head in the jaw joint area and a larger IP scale (*D. portschinskii*) (Fig. 6A; Supporting Information, Appendix S3A, B). The second axis (CV2) reflects differences in the shape of the frontal (Fr) and IP scales (Fig. 6B). Individuals with lower CV2 scores (*D. valentini*) have wider and shorter Fr and narrower IP scales (here, we consider the opposite directions of the CV axes produced by PC_CVA and LM_CVA), whereas individuals with higher scores have narrower and more elongated Fr and wider IP scales (*D. portschinskii*) (Fig. 6B; Supporting Information, Appendix S3A, B). The third CV axis mainly reflects differences in the configuration of the scales on the ventral head, in which *D. r. obscura* (lower scores) was partly differentiated from the rest (Fig. 6C; Supporting Information, Appendix S3C, D).

In 2D GM outline shape analysis, the NP-MANOVA also showed significant differences when *D. r. obscura* was treated as a separate taxon ($F_{3,48} = 4.4$; $P < 0.05$). However, post-hoc tests failed to differentiate *D. portschinskii* from *D. r. rudis* and *D. valentini*, or *D. valentini* from *D. r. obscura*. After Bonferroni correction, only *D. r. rudis* and *D. r. obscura* remained significantly different from each other. The CVA based on the seven 'meaningful' PCs generated three components explaining 51.7, 34.2 and 14.1% of the total variation; however, all taxa still partly overlapped along these axes (results not shown). The confusion matrix classified only 65% of the individuals correctly; after jackknifing, the precision of classification went down to 49% of the individuals (see Supporting Information, Appendix S5).

DISCUSSION

This paper suggests that a 3D analysis of head shape might provide important information not accessible using 'traditional' morphometrics or 2D GM, enabling separation of even very closely related species of lizards that are otherwise difficult to differentiate. Our study also suggests that the taxon *D. r. obscura* is morphometrically distinct from *D. r. rudis*, and there are sufficient reasons to qualify it as a separate species, *Darevskia obscura*.

The example considered in this paper contributes both to the methodology of morphometric comparisons of existing species and to the general understanding of species boundaries. De Queiroz (2007) defined a species

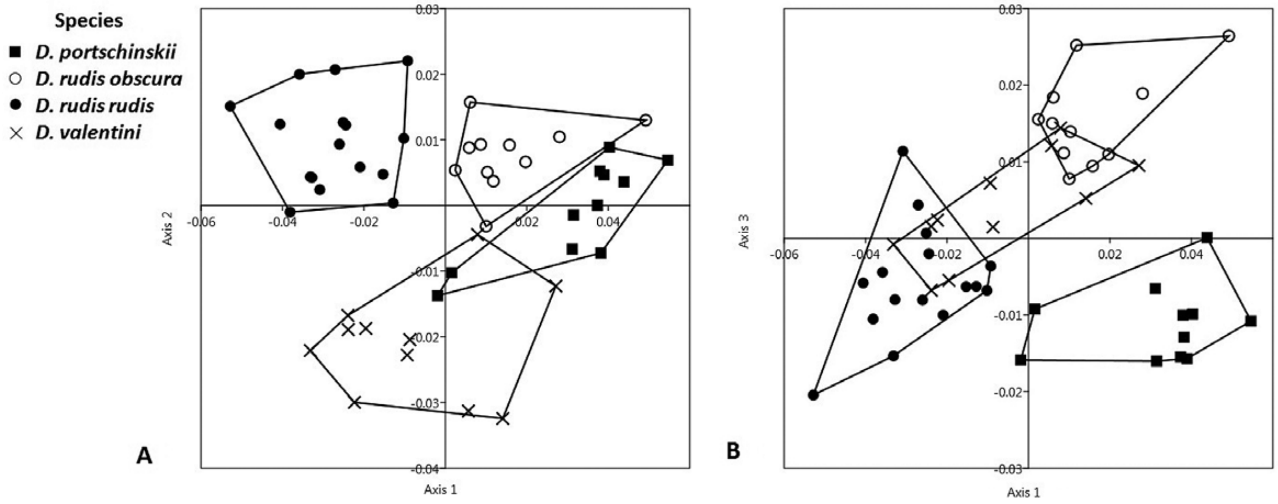

Figure 5. Plots of the between-group principal components analysis (BG-PCA) on the three-dimensional head shape of the *Darevskia* lizards, analysing all 66 landmarks. A, first vs. second axis. B, first vs. third axis.

as an evolutionary lineage with 'its own evolutionary pathway'. This definition acknowledges the fact that incipient species may hybridize and exchange alleles for a long period before achieving full reproductive isolation, which does not always prevent their divergence (Mallet, 2005). The studied nominal species of rock lizards did not achieve the stage of complete lineage sorting ('genealogical concordance' in terms of Avise & Ball, 1990) and, most probably, they continue to hybridize and show gene introgression patterns (Tarkhnishvili *et al.*, 2013). In the border areas, there are multiple individuals that cannot be allocated easily to either of the taxa, based solely on superficial examination (D. Tarkhnishvili, unpublished observations) or even study of the scalation pattern (Darevsky, 1967; Tarkhnishvili *et al.*, 2013).

Additionally, the nominal species have some characteristic features that apply to most of the populations or individuals. Adult specimens of *D. portschinskii* are almost always smaller than adult *D. r. rudis* or *D. r. obscura* from neighbouring locations. *Darevskia rudis obscura* adults are usually smaller than those of *D. r. rudis* from habitats with similar environmental conditions and reach higher elevations. *Darevskia valentini* has brighter dorsal coloration and smoother scales than most of the *D. rudis* populations, although some populations geographically intermediate between *D. valentini* and *D. r. obscura* (which Darevsky referred to as *D. r. macromaculata*) have individuals that are difficult to attribute to either nominal species [Arribas *et al.* (2013) even synonymized *D. r. macromaculata* with *D. r. obscura*]. Some specimens of the nominal species of the '*rudis*' clade show individual traits that are more similar to those of other species of the clade than to those of the species to which they belong. In this case, the geographical context should be considered before attributing these specimens to one or another taxon.

Our morphometric study showed that the vast majority of conspecific individuals are identifiable if the entire head shape is taken into account. Head shape helps to distinguish not only between nominal species (*D. rudis*, *D. portschinskii* and *D. valentini*) but also between them and a taxon previously considered to be a subspecies, *D. r. obscura*. Remarkably, the 2D GM outline analysis performed in the present study was unable to discriminate closely related species of the '*rudis*' clade, whereas 3D GM analysis could do so.

Several studies have shown 3D GM to be a powerful tool for differentiating reptilian taxa based on their head shape or head elements. Andjelković *et al.* (2016) differentiated closely related ring and dice snakes (*Natrix natrix* Linnaeus, 1758 and *Natrix tessellata* Laurenti, 1768) using 3D GM on the cranial elements. Three-dimensional GM was also able to differentiate significantly three Montpellier snakes: *Malpolon insignitus insignitus*, *Malpolon insignitus fuscus* (subspecies of *M. insignitus* Geoffroy Saint-Hilaire, 1827) and *Malpolon monspessulanus monspessulanus* (subspecies of *M. monspessulanus* Hermann, 1804) based on their head shape (Mangiacotti *et al.*, 2014). Three-dimensional GM has also been used for identifying fossil lizards (Gray *et al.*, 2017).

The head is a solid structure covered with easily recognizable large scales in Lacertids and some other lizards, making placement of homologous landmarks convenient. Consequently, 3D analysis of head shape is a good tool for taxonomic analysis based on morphology, much more reliable than 'traditional' analyses including a qualitative comparison of scalation, traditional morphometrics or GM based on the 2D images. Most

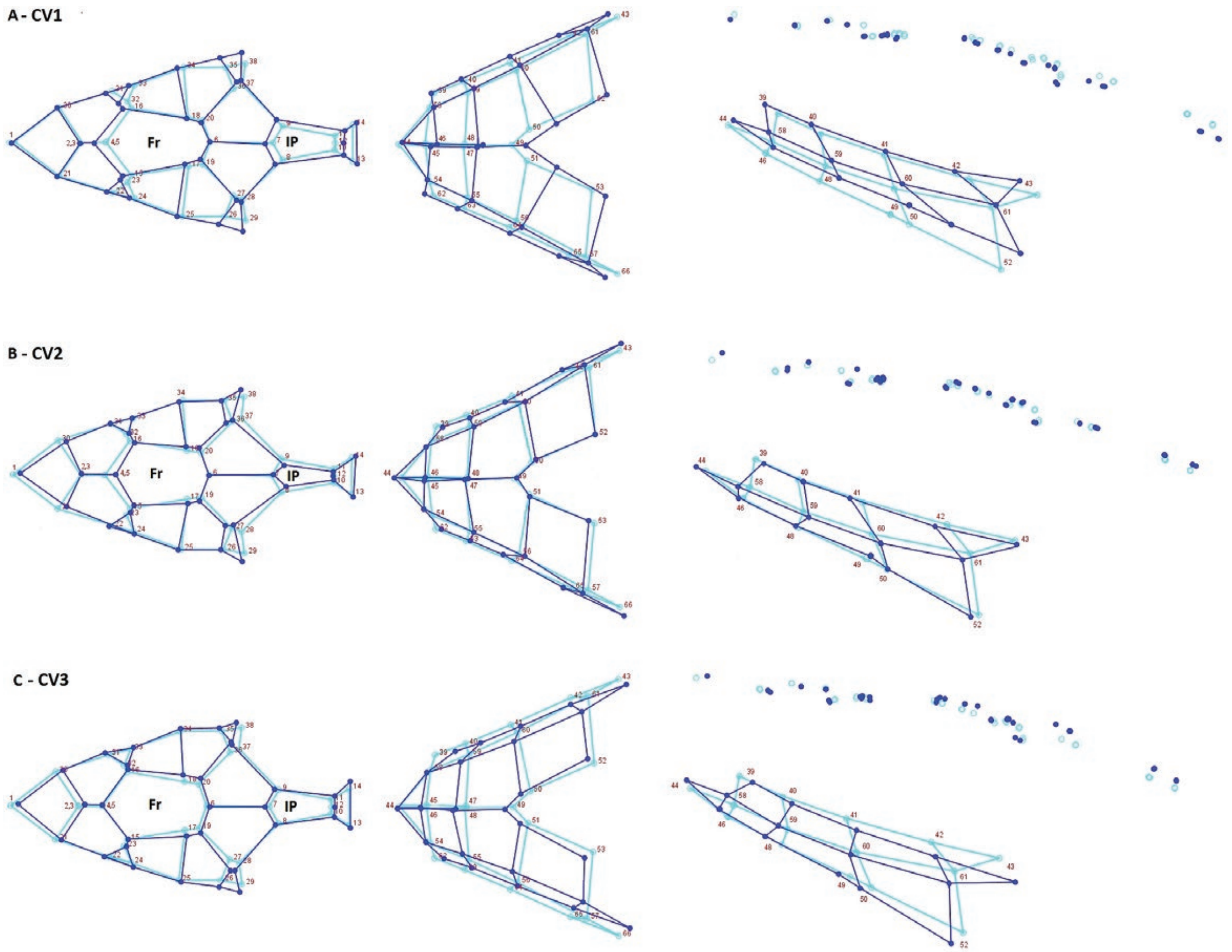

Figure 6. Wireframes for three canonical variate (CV) axes for visualizing shape changes. Dorsal, ventral and jaw wireframes (dots above the jaw wireframe are dorsal landmarks) from left to right. A–C, shape changes along the first (A), second (B) and third (C) CV axis. Light blue dots and lines represent the shape corresponding to the mean values along the respective CV axis. Dark blue dots and lines represent the shape corresponding to the maximal values along a respective CV axis, extrapolated up to 10.0 units to emphasize the subtle changes in shape.

importantly, it helps to discriminate even between species that did not achieve the stage of complete lineage sorting and individuals collected from the populations where molecular genetic analysis suggests the presence of introgressive gene flow (Tarkhnishvili *et al.*, 2013). Such individuals are commonly impossible to attribute to one or another species based on a limited number of genetic characters. However, 3D GM is able to cluster even these individuals with the other members of the same population.

TAXONOMIC INFERENCE

This morphometric study suggests that the populations of *D. rudis* from the upper part of the river Kura Valley, from the Borjomi Gorge southwards and west to the Goderdzi Pass, which Darevsky (1967) described as subspecies *D. r. obscura* and *D. r. macromaculata*, are morphologically not less distinct from *D. r. rudis* than the nominal species *D. valentini* and *D. portschinskii*. Different from *D. r. rudis*, the head of *D. r. obscura* is flatter but broader in the jaw joint area. It also has a relatively larger intraparietal scale than *D. r. rudis*. The earlier study of Tarkhnishvili *et al.* (2013) suggests that this form has a monophyletic matrilineal origin independent from the other *D. rudis* populations, and it is intermediate between *D. r. rudis*, *D. valentini* and *D. portschinskii* with respect to the distribution of microsatellite genotypes. This, however, does not apply to other populations of *D. rudis* (Tarkhnishvili *et al.*, 2013). Consequently, and following the original suggestion of Lantz & Cyrén (1936) who described this lizard as a subspecies of *D.* '*saxicola*' Eversmann, 1834 (that comprised most of the currently described species of *Darevskia*) and not of *D. rudis*, we suggest reinstating the status of this form to a species, *Darevskia obscura* Lantz & Cyrén, 1936.

ACKNOWLEDGEMENTS

The research was financed by Shota Rustaveli National Science Foundation of Georgia (Award #PhDF2016_79). We thank Ilia State University and Ghent University for providing technical support to this research; Mikheil Elashvili and Giorgi Datunashvili for assisting with the software Agisoft. Giorgi Iankoshvili and Natia Barateli assisted in the sample collection. The authors thank three anonymous reviewers for useful comments and suggestions.

REFERENCES

Abdel-Rahman EH, Taylor PJ, Contrafatto G, Lamb JM, Bloomer P, Chimimba CT. 2009. Geometric craniometric analysis of sexual dimorphism and ontogenetic variation: a case study based on two geographically disparate species, *Aethomys ineptus* from southern Africa and *Arvicanthis niloticus* from Sudan (Rodentia: Muridae). *Mammalian Biology-Zeitschrift für Säugetierkunde* **74:** 361–373.

Adams DC, Rohlf FJ, Slice DE. 2013. A field comes of age: geometric morphometrics in the 21st century. *Hystrix, the Italian Journal of Mammalogy* **24:** 7–14.

Agisoft LLC. 2016. *AgiSoft PhotoScan Professional (Version 1.2.6).* St. Petersburg: Agisoft LLC.

Andjelković M, Tomović L, Ivanović A. 2016. Variation in skull size and shape of two snake species (*Natrix natrix* and *Natrix tessellata*). *Zoomorphology* **135:** 243–253.

Arribas O, Ilgaz Ç, Kumlutaş Y, Durmuş SH, Avci A, Üzüm N. 2013. External morphology and osteology of *Darevskia rudis* (Bedriaga, 1886), with a taxonomic revision of the Pontic and Small-Caucasus populations (Squamata: Lacertidae). *Zootaxa* **3626:** 401–428.

Avise JC, Ball RMJ. 1990. Principles of genealogical concordance in species concepts and biological taxonomy. In: Futuyma D, Antonovics J, eds. *Oxford surveys in evolutionary biology*. New York: Oxford University Press, 45–67.

Bernal V. 2007. Size and shape analysis of human molars: comparing traditional and geometric morphometric techniques. *HOMO: Internationale Zeitschrift fur die vergleichende Forschung am Menschen* **58:** 279–296.

Blanco MB, Godfrey LR. 2006. Craniofacial sexual dimorphism in *Alouatta palliata*, the mantled howling monkey. *Journal of Zoology* **270:** 268–276.

Breno M, Leirs H, Van Dongen S. 2011. Traditional and geometric morphometrics for studying skull morphology during growth in *Mastomys natalensis* (Rodentia: Muridae). *Journal of Mammalogy* **92:** 1395–1406.

Cooley WW, Lohnes PR. 1971. *Multivariate data analysis*. New York: J. Wiley and Sons Inc.

Darevsky IS. 1967. *Rock lizards of the Caucasus: systematics, ecology and phylogenesis of the polymorphic groups of Caucasian rock lizards of the subgenus Archaeolacerta*. Leningrad: Nauka.

De Queiroz K. 2007. Species concepts and species delimitation. *Systematic Biology* **56:** 879–886.

Gabelaia M, Adriaens D, Tarkhnishvili D. 2017. Phylogenetic signals in scale shape in Caucasian rock lizards (*Darevskia* species). *Zoologischer Anzeiger-A Journal of Comparative Zoology* **268:** 32–40.

Goricki S, Trontelj P. 2006. Structure and evolution of the mitochondrial control region and flanking sequences in the European cave salamander *Proteus anguinus*. *Gene* **378:** 31–41.

Gray JA, McDowell MC, Hutchinson MN, Jones ME. 2017. Geometric morphometrics provides an alternative approach for interpreting the affinity of fossil lizard jaws. *Journal of Herpetology* **51:** 375–382.

Hammer Ø, Harper DA, Ryan PD. 2001. PAST: paleontological statistics software package for education and data analysis. *Palaeontologia Electronica* **4:** art. 4.

Ivanovic A, Aljancic G, Arntzen JW. 2013. Skull shape differentiation of black and white olms (*Proteus anguinus anguinus* and *Proteus a. parkelj*): an exploratory analysis with micro-CT scanning. *Contributions to Zoology* **82:** 107–114.

Jackson DA. 1993. Stopping rules in principal components analysis: a comparison of heuristical and statistical approaches. *Ecology* **74:** 2204–2214.

Kaliontzopoulou A, Carretero MA, Llorente GA. 2007. Multivariate and geometric morphometrics in the analysis of sexual dimorphism variation in *Podarcis* lizards. *Journal of Morphology* **268:** 152–165.

Klingenberg CP. 2011. MORPHOJ: an integrated software package for geometric morphometrics. *Molecular Ecology Resources* **11:** 353–357.

Klingenberg CP. 2013. Visualizations in geometric morphometrics: how to read and how to make graphs showing shape changes. *Hystrix, the Italian Journal of Mammalogy* **24:** 15–24.

Lantz LA, Cyrén O. 1936. Contribution à la connaissance de *Lacerta saxicola* Eversmann. *Bulletin de la Société zoologique de France* **61:** 159–181.

Maderbacher M, Bauer C, Herler J, Postl L, Makasa L, Sturmbauer C. 2008. Assessment of traditional versus geometric morphometrics for discriminating populations of the *Tropheus moorii* species complex (Teleostei: Cichlidae), a Lake Tanganyika model for allopatric speciation. *Journal of Zoological Systematics and Evolutionary Research* **46:** 153–161.

Mallet J. 2005. Hybridization as an invasion of the genome. *Trends in Ecology & Evolution* **20:** 229–237.

Mangiacotti M, Limongi L, Sannolo M, Sacchi R, Zuffi MA, Scali S. 2014. Head shape variation in eastern and western Montpellier snakes. *Acta Herpetologica* **9:** 167–177.

Microsoft Corporation. 2007. *Microsoft Office Excel (Version 12.0.4518.1014).* Redmond: Microsoft Corporation.

Murphy RW, Fu J, MacCulloch RD, Darevsky IS, Kupriyanova LA. 2000. A fine line between sex and unisexuality: the phylogenetic constraints on parthenogenesis in lacertid lizards. *Zoological Journal of the Linnean Society* **130:** 527–549.

Rohlf FJ, Marcus LF. 1993. A revolution morphometrics. *Trends in Ecology & Evolution* **8:** 129–132.

Schwarzfeld MD, Sperling FAH. 2014. Species delimitation using morphology, morphometrics, and molecules: definition of the *Ophion scutellaris* Thomson species group, with descriptions of six new species (Hymenoptera, Ichneumonidae). *ZooKeys* **462:** 59–114.

Sztencel-Jabłonka A, Jones G, Bogdanowic ZW. 2009. Skull morphology of two cryptic bat species: *Pipistrellus pipistrellus* and *P. pygmaeus* — a 3D geometric morphometrics approach with landmark reconstruction. *Acta Chiropterologica* **11:** 113–126.

Tarkhnishvili D. 2012. Evolutionary history, habitats, diversification, and speciation in Caucasian rock lizards. *Advances in Zoology Research* **2:** 79–120.

Tarkhnishvili D, Murtskhvaladze M, Gavashelishvili A. 2013. Speciation in Caucasian lizards: climatic dissimilarity of the habitats is more important than isolation time. *Biological Journal of the Linnean Society* **109:** 876–892.

Zelditch ML, Swiderski DL, Sheets HD, Fink WL. 2004. *Geometric morphometrics for biologists: a primer*. New York: Elsevier Ltd.

SUPPORTING INFORMATION

Additional Supporting Information may be found in the online version of this article at the publisher's web-site:

Appendix S1. Description of landmarks.
Appendix S2. Eigenvalues and character loadings for general principal components analysis (PCA) on three-dimensional shape data.
Appendix S3. Comparison of axes from canonical variate analysis based on seven meaningful principal components (PC_CVA) and canonical variate analysis based on the Procrustes coordinates of all 66 landmarks (LM_CVA). A, PC_CVA axis 1 vs. axis 2; B, LM_CVA axis 1 vs. axis 2; C, PC_CVA axis 1 vs. axis 3; D, LM_CVA axis 1 vs. axis 3.
Appendix S4. Upper panel, confusion matrix inferred from canonical variate analysis (CVA) assigning individuals to one of the four taxa based on the three-dimensional (3D) head shape. Lower panel, the jackknifed confusion matrix inferred from CVA assigning individuals to one of the four taxa based on the 3D head shape.
Appendix S5. Upper panel, confusion matrix inferred from canonical variate analysis (CVA) assigning individuals to one of the four taxa based on two-dimensional (2D) outline of anal scale. Lower panel, the jackknifed confusion matrix inferred from CVA assigning individuals to one of the four taxa based on 2D outline of the anal scale.